Analyst

Cite this: *Analyst*, 2012, **137**, 3132

www.rsc.org/analyst

PAPER

Sensitive and selective detection of glutathione based on resonance light scattering using sensitive gold nanoparticles as colorimetric probes†

Zhanguang Chen,*[a] Zhen Wang,[a] Junhui Chen,*[b] Shaobin Wang[c] and Xiaopeng Huang[a]

Received 26th March 2012, Accepted 19th April 2012
DOI: 10.1039/c2an35405e

In this paper, we reported the development of a highly sensitive and selective resonance light scattering (RLS) technique for glutathione using gold nanoparticle probes. The assay relies upon the distance-dependent optical properties of gold nanoparticles, the self-assembly of glutathione on gold nanoparticles, and the interaction of a 2 : 1 glutathione–Cu^{2+} complex. In the presence of Cu^{2+}, glutathione could rapidly induce the aggregation of gold nanoparticles, thereby resulting in greatly enhanced RLS intensity and red-to-blue (or purple) color change. The concentration of glutathione can be determined by the naked eye or a fluorescence spectrometer. Under the optical conditions, the detection of glutathione can be finished within 20 min, and the detection limit of 10 nM can be reached. The concentration range of the probe is 40–280 nM. The proposed method holds a specific selectivity toward glutathione and it is applied to the detection of glutathione in human serum with satisfactory results. In addition, the assay shows great potential application for disease-associated biomarkers, and it will meet the great demand for amino acid determination in fields such as food processing, biochemistry, pharmaceutical, and clinical analysis.

Introduction

Glutathione (γ-Glu-Cys-Gly, GSH) is the most abundant non-protein low molecular weight thiol source in most mammalian tissues.[1–3] This tripeptide naturally exists in two forms, one is reduced form (GSH) and another is oxidized dimeric form (GSSG) in the tissues which makes it perform as an important intracellular reduction–oxidation buffer.[4] Besides having the thiol/disulfide reduction–oxidation potential, GSH has many other crucial biological functions because the thiol redox state is involved in most major biologic processes.[5] It participates in the main redox potential maintaining system in eukaryotic cell homeostasis and prevents the oxidative stress and helps to trap free radicals that damage DNA and RNA.[6] There is evidence that oxidative stress contributes to the development of autism in children.[7] The oxidative stress has been implicated in many diseases and accelerates the aging process.[8] Recent studies have also suggested that the level of the tripeptide in plasma is related to diseases such as cancers, Alzheimer's disease, and Parkinson's disease.[8–17] Hence, the analysis of biomarkers of oxidative stress becomes the key factor for preventive treatments.

Due to the biological importance of GSH, the analysis of GSH is important, and the development of a new simple and accurate technique is desired. Currently, the determination of GSH is carried out using various detection techniques, including optical spectroscopy,[18–20] electrochemical pulse voltammetric methods,[21–23] and high-performance liquid chromatography.[24–26] However, several drawbacks, such as the lower selectivity against other amino acids due to their structural similarity, and the required cumbersome laboratory procedures, limit their clinical application.

The light scattering signals can be easily detected by synchronously scanning both the excitation and emission monochromators with a conventional spectrofluorometer.[27–31] Because the signal intensity is strongly dependent on the aggregation or assembly of samples, resonance light scattering (RLS) based assays have been used to detect nucleic acids,[32] adenine,[33] screen anticancer drugs,[34,35] and so on.[36–38] Recently, gold nanoparticle (AuNP) based RLS methods have been attracting enormous attention in biomolecules detection, since light scattering ability of AuNPs is about four orders of magnitude stronger than that of a fluorescent dye, *e.g.*, fluorescein.[39] In addition, the aggregations of AuNPs are often accompanied by distinct color changes. The well-dispersed AuNPs solution is red whereas aggregated AuNPs appear blue (or purple). The color change induced by the aggregation of AuNPs provides the basis for the colorimetric analysis.

[a]*Department of Chemistry, Shantou University, Shantou 515063, China. E-mail: kqlu@stu.edu.cn; Fax: +86 75482902767; Tel: +86 75482903330*
[b]*Interventional oncology & minimally invasive Therapies Department, Peking University Shenzhen Hospital, Shenzhen, 518036, China. E-mail: chenjupush@126.com; Tel: +86 13902732800*
[c]*Department of Oncology, the First Affiliated Hospital of Shantou University Medical College, Shantou, 515041, China*

† Electronic supplementary information (ESI) available. See DOI: 10.1039/c2an35405e

In this study, we reported the AuNPs as a probe for GSH. The thiol group of GSH tends to readily adsorb onto the surface of colloidal gold particles *via* Au–S bond; at the same time, a copper ion could bind with two GSH molecules.[40,41] Thus, copper ion can act as a cross-linking agent for pairs of GSH-coated AuNPs, thereby inducing the aggregation of AuNPs and red-to-blue (or purple) color change. As a result, the large size of assemblies of gold nanoparticles leads to strong RLS signals. Accordingly, a novel, rapid, simple and sensitive RLS method for the determination of GSH was proposed and applied to detect the GSH in human serum with satisfactory results.

Experimental

Reagents

Chloroauric acid ($HAuCl_4$) was purchased from Sinopharm Group Chemical Reagent Co., Ltd. Reagent Inc. Sodium citrate was purchased from Beijing Chemical Reagent Company (Beijing, China). All of the amino acids were purchased from rice Biotechnology Co. Ltd. and used without further purification. Cu^{2+} (10 mM) was prepared by dissolving some $CuSO_4$. Stock solution of GSH at 10^{-3} mol L^{-1} was prepared by dissolving the GSH in double distilled water and stored in a refrigerator at 4 °C. Working solutions were obtained by serially diluting the stock solution immediately prior to use. Double distilled water was used throughout all experiments. The human serum samples were obtained from healthy people in the Medical College, Shantou University (Shantou, China). The Britton–Robin (BR) buffer solution was used to control the acidity of the solution, which was made up of 0.04 mol L^{-1} phosphoric acid, 0.04 mol L^{-1} acetic acid, 0.04 mol L^{-1} boric acid, and 0.2 mol L^{-1} sodium hydroxide.

Apparatus

The RLS spectra were recorded on a LS-55 fluorescence spectrophotometer (Perkin-Elmer, USA) equipped with a 1 cm × 1 cm quartz cuvette at room temperature. All absorption spectra were recorded on a Lambda 950 UV-vis Spectrophotometer (PerkinElmer, USA) at room temperature. The SEM images were obtained on a JEOL-JSM6360LA scanning electron microscope. The photographs were taken with a Cannon SX230 digital camera. All pH measurements were made with a DELTA 320-S acidity meter (Mettler-Toledo Instruments Co. Ltd., Shanghai, China).

General experimental procedure

Preparation of gold nanoparticles (AuNPs). All glassware used in the following procedure was cleaned in a bath of freshly prepared chromate washings (cleansing solution), rinsed thoroughly in water and dried in air. AuNPs were prepared according to the published protocol.[42] Briefly, after boiling 100 mL of 0.01% $HAuCl_4$ solution, 3.5 mL of 1.0% trisodium citrate solution was quickly added with vigorous stirring. The mixed solution was boiled for 10 min and further stirred for 15 min. After the solution was naturally cooled to room temperature, it was filtered through a 0.32 μm membrane filter and stored in the refrigerator (4 °C) and ready for use. The resulting solution of colloidal particles was characterized by absorption maximum at 520 nm. The solution was diluted with water until its absorbance at 520 nm was equal to 1.000. We denote the concentration of the resulting solution of AuNPs to be 1×.

RLS spectra. First, 0.5 mL BR (pH 7.0) buffer and 2.5 mL AuNPs were added into a 10 mL calibrated flask, and then mixed with a certain amount of GSH solution. This solution was allowed to react for 5 min.[43] Next, 0.5 mL (0.01 M) Cu^{2+} was added to the above prepared solution, the mixture was finally diluted to 5 mL with doubly distilled water, then the solution was allowed to react for 20 min at room temperature. RLS spectra were obtained by scanning synchronously with the same excitation and emission wavelength ($\lambda_{ex} = \lambda_{em}$) from 200 to 700 nm. Both the excitation and emission slit widths were kept at 10.0 nm. The enhanced RLS intensity of AuNPs was represented as $\Delta I_{RLS} = I_{RLS} - I^0_{RLS}$ and I_{RLS} and I^0_{RLS} were RLS intensities of the AuNPs with and without GSH.

UV-vis spectra. UV-vis absorbance spectra were obtained by a Lambda 950 UV-vis spectrophotometer (Perkin Elmer, USA) equipped with a quartz micro-colorimetric vessel of 1 cm path length. In the UV-vis assay, the preparation of solutions was the same as in the RLS spectra method. And the scanning range was from 200 nm to 800 nm.

SEM measurement. The SEM samples were prepared by directly dripping the solutions on a cover glass which had been washed thoroughly with 95% ethanol. And then the samples were scanned on a JEOL-JSM6360LA scanning electron microscope.

Detect GSH in diluted human serum. The similar detection procedure was used as described in aqueous solution, except that diluted human serum was applied as the reaction matrix. The diluted human serum was prepared by adding 1 mL fresh human serum into the 99 mL BR buffer samples, and mixed well. The GSH spiked diluted human serum samples were prepared by adding different amounts of GSH into the as-prepared diluted human serum and mixed well.

Results and discussion

Characteristics of the light scattering spectra

Fig. 1 shows the light scattering spectra of gold nanoparticles and the conjugated gold nanoparticles with different concentrations of GSH and 1 mmol L^{-1} Cu^{2+}. The diameter of the AuNPs is approximately 16 nm, which is less than 1/20 of the incident light wavelength. Therefore, the light scattering of AuNPs can be considered the RLS.[44] From Fig. 1, it can be seen that the gold nanoparticles have a very weak RLS signal when they exist in aqueous solution alone. However, when the GSH and 1 mmol L^{-1} Cu^{2+} were added into the solution, the RLS intensity was remarkably enhanced. Fig. 1 also shows that the enhanced RLS intensities continuously increase with a gradual increase in the GSH concentration, while the spectral profile is maintained almost the same. These situations contribute to the fact that the AuNPs aggregate after addition of GSH and Cu^{2+}. To compare the light scattering spectra of AuNPs with those of AuNPs–GSH

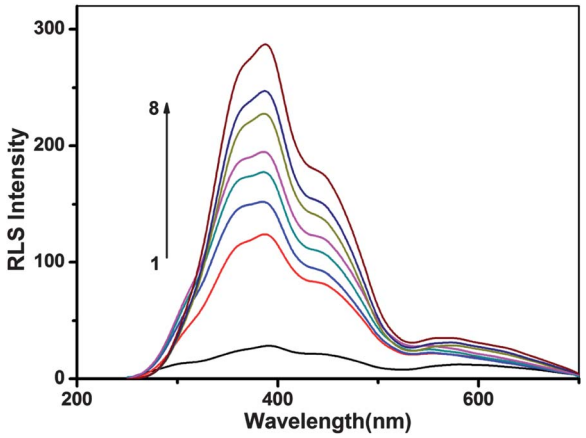

Fig. 1 RLS spectra of AuNPs (1) in the absence of GSH, (2–8) and in the presence of 40, 80, 120, 160, 200, 240, 280 nmol L^{-1} GSH and 1.0 mmol L^{-1} Cu^{2+}. *Conditions*: 0.5× AuNPs, BR (pH 7.0) buffer solution.

conjugates, it can be concluded that the assembly of AuNPs results in great enhancement of RLS intensity of AuNPs. On the other hand, the assembly of AuNPs *via* GSH leads to the size increases of scatters, which results in the RLS enhancement.

Sensor operation principle

Scheme 1 illustrates the analytical process for detecting GSH. In the absence of GSH, AuNPs in aqueous solution are stabilized against aggregation due to the negative capping agent's (citrate ions) electrostatic repulsion against van der Waals attraction between AuNPs,[45] and it has very weak RLS intensity and appears red. After addition of GSH, the thiol group of GSH exhibits intriguing reactivity with AuNPs. GSH binds onto the gold surface through the sulfur atom,[40,46] and the AuNPs are thus functionalized with GSH. Then, adding Cu^{2+} into the solution, GSH can bind Cu^{2+} by coordination with its acidic (COOH) and basic (NH_2) functional groups.[47–49] Each Cu^{2+} is chelated by two GSH molecules as shown schematically in Scheme 1. This four coordinate complexation of copper is entirely consistent with the preferred tetragonal geometry of complexed Cu^{2+}.[50] Thus, Cu^{2+} can act as a cross-linker for pairs of GSH-coated AuNPs, thereby inducing the aggregation of AuNPs which leads to the greatly enhanced RLS intensity. In addition, it also causes a rapid, red-to-blue (or purple) color change. We just make use of this property to design our sensor for GSH.

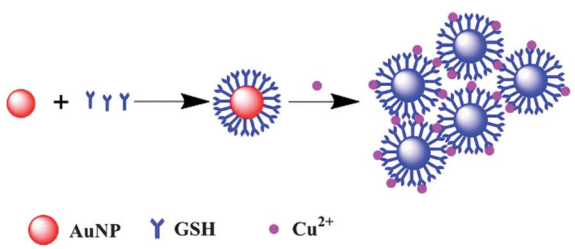

Scheme 1 Schematic representation of the analytical process for detecting GSH.

Colorimetric detection of GSH

Shown in Fig. 2 is a typical colorimetric detection of GSH using unmodified AuNPs probes. From Fig. 2, we can see that the color of AuNPs colloidal solution is red, while the AuNPs colloidal solution with Cu^{2+} in the presence of GSH (10^{-7} mol L^{-1}) is purple; as the concentration of GSH increases from 10^{-7} mol L^{-1} to 10^{-6} mol L^{-1}, the color of AuNPs solution changes from purple to blue.

Validation test

Additionally, in order to identify the form of the AuNPs without and with GSH, the SEM images (Fig. 3) were obtained. Note that in the absence of GSH, the AuNPs were dispersed (Fig. 3A); while in the presence of GSH with Cu^{2+}, the AuNPs aggregated together (Fig. 3B). The result was consistent with UV-vis absorption spectra. As shown in Fig. 4, the absorption spectrum (curve b) in Fig. 4 has two peaks: one is centered at ~520 nm, which is ascribed to the surface plasmon resonance absorption corresponding to the dispersed AuNPs; the other is centered at ~660 nm, which is ascribed to the absorption from the aggregated AuNPs.[43,48] It is just because of the electric dipole–dipole interaction and coupling between the plasmons of neighboring particles in the formed aggregates.[51] Hence, the experiments above have a consistent result; they confirmed that the principle of the sensor is reasonable.

Optimization of assays

With a fixed strategy, the performance of the developed sensing for GSH is still influenced by the assay conditions such as media pH, AuNPs concentration, binding time, metal ions species and metal ions concentration. Different assay conditions were investigated in our studies.

Effect of pH. Media pH not only affects the interaction between AuNPs and GSH, but also influences GSH–Cu^{2+} binding. The effect of pH on the response of the AuNPs probe was carried out at a pH range from 3.5 to 8.8. The RLS intensity *versus* media pH was obtained by adjusting media pH with different concentration ratios of acid to base and fixing the GSH concentration at 200 nM. As Fig. S1 (ESI†) shows, the RLS intensity of AuNPs as a blank decreases slowly with the increasing pH of the solution. With the increase of pH, the ionization of the –COOH group in citric acids on the gold nanoparticle surface increases, and in turn the negative charges

Fig. 2 Photographs of a solution of (1) 0.5× AuNPs + 1 mmol L^{-1} Cu^{2+}, (2) 0.5× AuNPs + GSH (10^{-7} mol L^{-1}) +1 mmol L^{-1} Cu^{2+}, (3) 0.5× AuNPs + GSH (10^{-6} mol L^{-1}) + 1 mmol L^{-1} Cu^{2+}. *Experimental conditions*: 0.5 mL BR (pH 7.0) buffer solution and diluted to 5 mL with water.

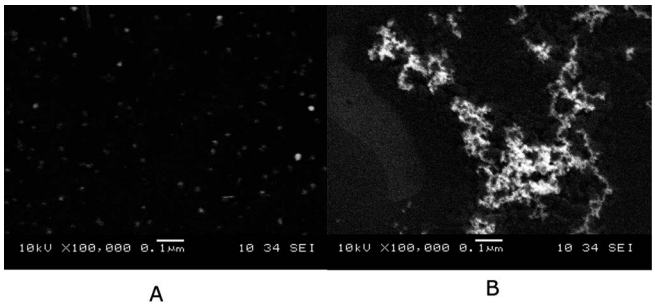

Fig. 3 Typical SEM images of (A) 0.5× AuNPs, (B) 0.5× AuNPs + 200 nmol L^{-1} GSH + 1.0 mmol L^{-1} Cu^{2+} in BR (pH 7.0) buffer solution.

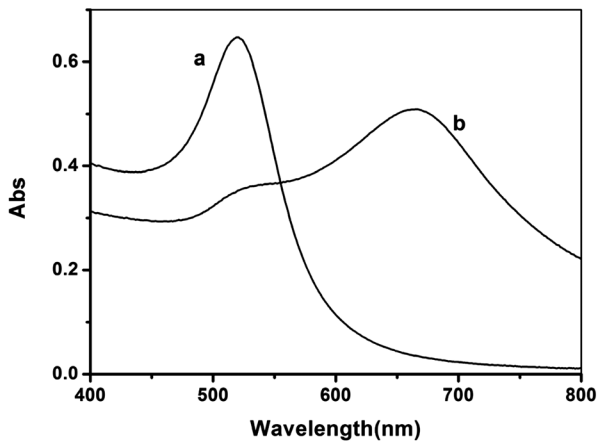

Fig. 4 UV-vis absorption spectra of (a) 0.5× gold nanoparticles and (b) 0.5× gold nanoparticles + 200 nmol L^{-1} GSH + 1.0 mmol L^{-1} Cu^{2+}, BR (pH 7.0) buffer solution.

of the $-COO^-$ group increase.[52] As a result, the electrostatic repulsion among AuNPs becomes stronger, which leads to the increase in the degree of dispersion of AuNPs. Thus, according to the principle of RLS,[32] the RLS intensity of AuNPs as a blank decreases slowly with the increasing pH of the solution. On the other hand, the RLS intensity of AuNPs–GSH–Cu^{2+} conjugates greatly depends on the pH of the solution and reaches the maximum at pH 7.0. The experimental results showed that at low pH the RLS intensity of the system was obviously increased by adding GSH, but when some other amino acids (such as histidine, lysine, arginine, methionine, tyrosine) were added into the system, the RLS intensity was also greatly increased, which is due to the pK_a of the $-NH_3^+$ group that is 9–10, thus the amine group in these amino acids is positively charged (namely, $-NH_3^+$) and it can bind AuNPs at low pH, whereas, the thiol group (SH) can bind AuNPs at high pH (pH > 5.0).[40] That is, at high pH (>5.0), only GSH could induce the increment of RLS intensity and other amino acids have no effect on RLS intensity because of the thiol group in GSH. Thus, we could control the media pH in order that the thiol group of GSH would selectively bind AuNPs. In the case of high pH values (pH > 7.0), the RLS intensity of the system decreased with increasing pH value, probably because high pH would weaken the ligation of GSH to Cu^{2+}.[40] Thus, we chose pH = 7.0 BR buffer solution as the reaction media.

Effect of concentration of AuNPs. The AuNPs concentration also influenced the detection of GSH. The optimization curve for the AuNPs concentration is shown in Fig. S2 (ESI†). The RLS intensity of gold nanoparticles as a blank gradually increases with increasing AuNPs concentration. When the concentration of the AuNPs solution is varied from 0.1× to 0.8×, the RLS intensity of AuNPs–GSH–Cu^{2+} conjugates greatly increases from 0.1× to 0.5× and then decreases beyond 0.5×. The reason is listed below. When the concentration of AuNPs is too low, it is not enough for GSH with a high concentration. That is to say, some amount of GSH cannot be adsorbed onto the surface of AuNPs, thus the RLS intensity is very weak. In contrast, with the increase of the concentration of AuNPs (0.1× to ~0.5×), almost all the GSH molecules can be adsorbed onto the surface of the AuNPs. As a result, the RLS intensity of AuNPs–GSH–Cu^{2+} conjugates would increase. However, as the concentration of AuNPs increased continually (>0.5×), the density of GSH per AuNP would decrease. Although the addition of Cu^{2+} can result in the aggregation, the extent of aggregation is lower than it was previously (0.1× to 0.5×). Thus, the RLS intensity decreases when the concentration of AuNPs is beyond 0.5×. As shown in Fig. S2†, the RLS intensity of AuNPs–GSH at 0.4× was the same as that at 0.5×. However, when the concentration of AuNPs is too low, GSH with a high concentration cannot be accurately detected. Therefore, in this system, we used 0.5× AuNPs (approximately 16 nm) for all experiments. Moreover, a 16 nm diameter AuNP is composed of 8.4×10^4 gold atoms,[53] and the surface gold atom (per particle) is about 1.7×10^4. Namely, a 16 nm diameter gold nanoparticle can bind about 1.7×10^4 GSH molecules through the Au–S bond.[40] Moreover, the binding of AuNPs and GSH is very fast.[43] In this system, the amount of AuNPs is sufficient for the GSH. In order to validate the result above, the mixture solution of 0.5× AuNPs, 300 nM GSH, 1 mM Cu^{2+} and appropriate H_2O was prepared and incubated for 20 min, then the mixture solution was centrifuged. Based on the turn-on effect of GSH on the Hg^{2+}–gold nanocluster system,[54] we attempt to detect GSH in the supernatant with this method, and no free GSH was found in the system. Consequently, almost all GSH could be functionalized on the AuNPs when 0.5× AuNPs were used in the system.

Effect of ion species and concentration. The experiment showed that the AuNPs capped with GSH could not rapidly aggregate in the absence of Cu^{2+}. The features can be interpreted in relation to the surface charge distribution of the AuNPs. The aggregation of AuNPs requires a cross-linker. For GSH with a carboxyl terminal group, the GSH-capped AuNPs surface will still bear negatively charged ($-COO^-$) groups, which will block close approach of AuNPs. Then, a cross-linker is necessary for rapid aggregation of AuNPs. Some metal ions could be chelated with GSH, and each metal ion could bind two (or three) GSH molecules. So, the metal ion would be the bridge for cross-linking of AuNPs. As shown in Fig. S3 (ESI†), we studied the effect of many metal ions including Pb^{2+}, Cd^{2+}, Fe^{2+}, Co^{2+}, Ni^{2+}, Zn^{2+}, Mn^{2+}, Ca^{2+}, Mg^{2+}, Ba^{2+}, $Al^{3+}$and Fe^{3+} on the experiment. Among these metal ions, Cu^{2+} is better than other metal ions. The reason is that the chelation of GSH toward Cu^{2+} is effective and far superior to that towards any other metal ions. Therefore, we chose Cu^{2+} as the cross-linker in the experiment.

Furthermore, the Cu^{2+} concentration is also a key factor for this experiment. From Fig. S4 (ESI†), we can see that the Cu^{2+} with high concentration results in an increase of the background signal, which will reduce the sensitivity of the sensor. Thus, high concentration of Cu^{2+} is unsuitable for detection of the target. Therefore, from the results above, we could see that the optimum concentration of Cu^{2+} for the system was 1 mM.

Influence of temperature and time. The binding temperature influenced the response of the sensor. In the range of 20–45 °C, the ΔI decreased with increasing temperature. The possible reason is that high temperature could induce self-aggregation of the AuNPs and weaken the ligation of GSH to Cu^{2+}. Hence, room temperature (*ca.* 20 °C) was used for the detection temperature. An incubation time of AuNPs–GSH binding and GSH–Cu^{2+} binding is expected to yield an enhanced signal. From Fig. S5 (ESI†) we can see that for low concentration of GSH (40 nM) the RLS intensity reached a maximum in 20 min; for high concentration of GSH (280 nM), 10 min incubation time was enough for the system to reach equilibrium. Thus, in order to detect glutathione with high accuracy, we chose 20 min as the experimental time. Compared with the previously reported determination of GSH, the assay is more rapid.

Selectivity

To examine the high selectivity of the proposed sensor for GSH, other α-amino acids (including lysine, arginine, serine, isoleucine, valine, methionine, aspartic acid, leucine, histidine, phenylalanine, tryptophan, glycine, threonine, alanine) and other thiol compounds (including cysteine, thioglycolic acid and mercaptoethyl alcohol) were examined under identical conditions. The experimental results are shown in Fig. S6 (ESI†). It is clear that only 200 nM GSH could effectively induce a significant increase of ΔI_{RLS} intensity. For the other α-amino acids with concentrations of up to 0.5 mM, the ΔI_{RLS} was very small which could be ignored. This strongly demonstrates that other amino acids could not produce the wrong signals even if present at higher concentrations. This means that the assay responds selectively towards GSH.

There are two factors responsible for the high selectivity of this sensor. First, according to the literature,[55] GSH has stronger affinity for AuNPs due to the multidentate anchor. The specific steric structure existing in GSH renders the GSH molecule to encapsulate AuNPs in priority leaving little or no chance for other amino acids binding on the AuNPs. And the literature[55] also demonstrated that the coordination priority of GSH on AuNPs reduces the aggregation capacity of other reagents that co-exist. In addition, the selectivity of GSH from thiol compounds (such as cysteine) can be achieved by their different aggregation kinetics.[43,56] The aggregation change for cysteine exhibits a rate that is about three orders of magnitude higher than that for GSH.[43] That is to say, the addition of cysteine into AuNPs will quickly cause the aggregation of AuNPs. At this point, the GSH modified AuNPs were dispersed. Only as Cu^{2+} was added into the system, did the dispersed AuNPs aggregate immediately. Moreover, the quantitative of the assay is based upon the ΔI which is the *D*-value of RLS intensity after and before addition of the GSH. The influence of thiol compounds (such as cysteine) can also be eliminated by the *D*-value. Hence, the proposed assay has high selectivity for GSH among other amino acids.

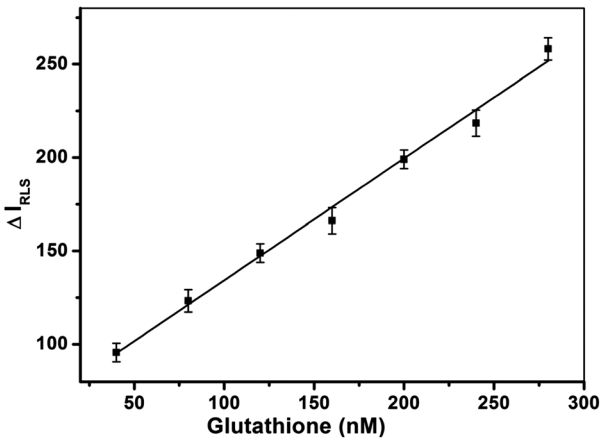

Fig. 5 The normalized curves between the increment of RLS intensity (ΔI) and the various concentrations of GSH.

Tuning dynamic range

A tunable dynamic range is important for practical applications as the desirable concentration for the same target analyte can be different for various applications. In this study, with the exception of the concentration of AuNPs, the size of AuNPs is also a critical factor for the detection. When the AuNPs concentration is low, it is very sensitive for detecting smaller amounts of GSH. Moreover, large AuNPs were more sensitive to GSH. But the selectivity of large AuNPs was not ideal. Therefore, considering the accuracy of detecting GSH, different kinds of AuNPs were chosen for practical applications.

Quantitative detection of GSH

As indicated in Fig. 1, the RLS intensity was sensitive to GSH and increased as the concentration of GSH increased. Under the optimum conditions, the calibration curve (Fig. 5) for the determination of GSH is constructed. There is a good linear relationship between the RLS intensity and the concentration of GSH in the range 40–280 nM. The standard regression equation is $\Delta I_{RLS} = 69.01 + 0.65C_{GSH}$ and the corresponding regression coefficient is 0.9929. The detection limit of GSH by this method was estimated on the basis of 3 times the blank test standard deviation and it is 10 nM. The result implied that this method showed a highly sensitive response to GSH.

Determination of GSH in human serum

To further demonstrate the applicability of the assay, it was applied to detect GSH in five different diluted human serum samples because of variations in the chemical composition of biological fluids. Using our method, the detection of GSH can be satisfactorily achieved. The recoveries of these measurements are in the range of 98.85–102.86% under the optimal conditions (as shown in Table 1), indicating that this method is reliable and practical.

Table 1 Results of determination of GSH in human serum samples using the RLS method

Sample number	GSH (added)/ nmol L^{-1}	GSH (detected)/ nmol L^{-1}	Recovery (%)	RSD (%, $n = 5$)
1	50	48	98.85	5.25
2	70	72	100.86	4.80
3	100	98	99.56	2.13
4	150	148	99.67	3.67
5	200	203	102.86	1.58

Conclusions

In this work, combining the unique RLS property of AuNPs and special interaction of GSH with Cu^{2+}, a novel RLS assay has been developed for detecting GSH. The novel RLS based method offers a wide concentration range of 40 to 280 nM with a limit of detection of 10 nM for GSH. Compared with the previously reported detection methods, our approach is simple and it has reasonable sensitivity and selectivity. Furthermore, one of the significant features of the present system is its ability to detect GSH by monitoring the color change with naked eye. Furthermore, our protocol provides a good selectivity for various other α-amino acids and some other thiol compounds. Otherwise, the dynamic range of this sensor can be tuned simply by adjusting the concentration and size of AuNPs, which can impart the sensor with a wide range of applications.

Acknowledgements

All authors gratefully acknowledge the financial support of the Natural Science Foundation of Guangdong Province (9151022501000019).

References

1 A. Meister and M. E. Anderson, *Annu Rev Biochem*, 1983, **52**, 711–760.
2 M. Novak and J. Lin, *J. Am. Chem. Soc.*, 1996, **118**, 1302–1308.
3 E. M. Kosower, in *Coenzyme and Cofactors Volume III: GSH*, ed. D. Dolphin, R. Poulson and O. Avramovic, Wiley, New York, 1989, Part A, p. 103.
4 B. Noszal and Z. Szakacs, *J. Phys. Chem. B*, 2003, **107**, 5074–5080.
5 O. Lampela, A. H. Juffer and A. Rauk, *J. Phys. Chem. A*, 2003, **107**, 9208–9220.
6 C. K. Mathews, K. E. van Holde and K. G. Ahem, *Biochemistry*, Addison Wesley Longman, San Fransisco, 3rd edn, 2000.
7 A. Chauhan and V. Chauhan, *Pathophysiology*, 2006, **13**, 171–181.
8 F. J. Giblin, *J. Ocul. Pharmacol. Ther.*, 2000, **16**, 121–135.
9 H. Liu, H. Wang, S. Shenvi, T. M. Hagen and R.-M. Liu, *Ann. N. Y. Acad. Sci.*, 2004, **1019**, 346–349.
10 P. Miao, L. Liu, Y. J. Nie and G. X. Li, *Biosens. Bioelectron.*, 2009, **24**, 3347–3351.
11 W. Zhang, F. L. Wang, W. Zhu, H. H. Xu, X. Y. Ye, R. Y. Cheng and L. T. Jin, *J. Chromatogr. B*, 2005, **818**, 227–232.
12 P. C. White, N. S. Lawrence, J. Davis and R. G. Compton, *Electroanalysis*, 2002, **14**, 89–98.
13 N. S. Lawrence, R. P. Deo and J. Wang, *Talanta*, 2004, **63**, 443–449.
14 H. Refsum, A. D. Smith, P. M. Ueland, E. Nexo, R. Clarke, J. Mcpartlin, C. Johnston, F. Engbaek, J. Schneede, C. Mcpartlin and J. M. Scott, *Clin. Chem.*, 2004, **50**, 3–32.
15 H. Refsum, P. M. Ueland, O. Nygard and S. E. Vollset, *Annu. Rev. Med.*, 1998, **49**, 31–62.
16 S. Seshadri, A. Beiser, J. Selhub, P. F. Jacques, I. H. Rosenberg, R. B. D'Agostino, P. W. F. Wilson and P. A. Wolf, *N. Engl. J. Med.*, 2002, **346**, 476–483.
17 W. A. Kleinman and J. P. Richie, *Biochem. Pharmacol.*, 2000, **60**, 19–29.
18 O. Rusin, N. N. S. Luce, R. A. Agbaria, J. O. Escobedo, S. Jiang, I. M. Warner, F. B. Dawan, K. Lian and R. M. Strongin, *J. Am. Chem. Soc.*, 2004, **126**, 438–439.
19 W. H. Wang, O. Rusin, X. Y. Xu, K. K. Kim, J. O. Escobedo, S. O. Fakayode, K. A. Fletcher, M. Lowry, C. M. Schowalter, C. M. Lawrence, F. R. Fronczek, I. M. Warner and R. M. Strongin, *J. Am. Chem. Soc.*, 2005, **127**, 15949–15958.
20 F. Tanaka, N. Mase and C. F. Barbas III, *Chem. Commun.*, 2004, 1762–1763.
21 N. Spataru, B. V. Sarada, E. Popa, D. A. Tryk and A. Fujishima, *Anal. Chem.*, 2001, **73**, 514–519.
22 J. C. Ndamanisha, J. Bai, B. Qi and L. P. Guo, *Anal. Biochem.*, 2009, **386**, 79–84.
23 M. Stobiecka, J. Deeb and M. Hepel, *J. Electrochem. Soc.*, 2009, **19**, 15–32.
24 C. Lu, Y. B. Zu and V. W. W. Yam, *J. Chromatogr., A*, 2007, **1163**, 328–332.
25 W. Zhang, F. L. Wan, W. Zhu, H. H. Xu, X. Y. Ye, R. Y. Cheng and L.-T. Jin, *J. Chromatogr., B: Anal. Technol. Biomed. Life Sci.*, 2005, **818**, 227–232.
26 J. Vacek, B. Klejdus, J. Petrlova, L. Lojkova and V. Kuban, *Analyst*, 2006, **131**, 1167–1174.
27 R. F. Pasternack, C. Bustamante, P. J. Colling, A. Giannetto and E. J. Gibbs, *J. Am. Chem. Soc.*, 1993, **115**, 5393–5399.
28 R. F. Pasternack, C. Bustamante and P. J. Collings, *Science*, 1995, **26**, 9935–9939.
29 S. K. Brar and M. Verma, *TrAC, Trends Anal. Chem.*, 2011, **30**, 4–17.
30 L. Ling, C. Z. Huang, Y. F. Li, L. Zhang, L. Q. Chen and S. J. Zhen, *TrAC, Trends Anal. Chem.*, 2009, **28**, 447–453.
31 J. Ling, C. Z. Huang, Y. F. Li, Y. F. Long and Q. G. Liao, *Appl. Spectrosc. Rev.*, 2007, **42**, 177–201.
32 C. Z. Huang, K. A. Li and S. Y. Tong, *Anal. Chem.*, 1996, **68**, 2259–2263.
33 Q. Y. Xu, Z. F. Liu, X. L. Hu, L. Kong and S. P. Liu, *Analyst*, 2012, **137**, 868–874.
34 Z. G. Chen, T. H. Song, S. B. Wang, X. Chen, J. H. Chen and Y. Q. Li, *Biosens. Bioelectron.*, 2010, **25**, 1947–1952.
35 Z. G. Chen, Y. R. Peng, M. H. Chen, X. Chen, J. H. Chen and G. M. Zhang, *Analyst*, 2010, **135**, 2653–2660.
36 Z. G. Chen, G. M. Zhang, X. Chen, J. H. Chen, S. H. Qian and Q. Li, *Analyst*, 2012, **137**, 722–728.
37 Z. G. Chen, T. H. Song, Y. R. Peng, X. Chen, G. M. Zhang and S. H. Qian, *Analyst*, 2011, **136**, 3927–3933.
38 Z. G. Chen, G. M. Zhang, X. Chen and W. H. Gao, *Anal. Bioanal. Chem.*, 2012, **402**, 2163–2171.
39 L. Li and B. X. Li, *Analyst*, 2009, **134**, 1361–1365.
40 Q. Dai, X. Liu, J. Coutts, L. Austin and Q. Huo, *J. Am. Chem. Soc.*, 2008, **130**, 8138–8139.
41 K. C. Grabar, R. G. Freeman, M. B. Hommer and M. J. Natan, *Anal. Chem.*, 1995, **67**, 735–743.
42 C. C. Huang, Y. F. Huang, Z. H. Cao, W. H. Tan and H. T. Chang, *Anal. Chem.*, 2005, **77**, 5735–5741.
43 F. X. Zhang, L. Han, L. B. Israel, J. G. Daras, M. M. Maye, N. K. Ly and C. J. Zhong, *Analyst*, 2002, **127**, 462–465.
44 G. A. Miller, *J. Phys. Chem.*, 1978, **82**, 616–618.
45 A. Ono and H. Togashi, *Angew. Chem., Int. Ed.*, 2004, **43**, 4300–4302.
46 K. Uvdal, P. Bodo and B. J. Liedberg, *Adv Colloid Interface Sci*, 1992, **149**, 162–173.
47 A. C. Liu, D. C. Chen, C. C. Lin, H. H. Chou and C. H. Chen, *Anal. Chem.*, 1999, **71**, 1549–1552.
48 W. B. Chen, X. J. Tu and X. Q. Guo, *Chem. Comm.*, 2009, 1736–1738.
49 F. Cheng and X. Y. Zhou, *Electroanalysis*, 2003, **15**, 1632–1638.
50 H. Sigel and R. B. Martin, *Chem. Rev.*, 1982, **82**, 385–426.
51 U. Kreibig and L. Genzal, *Surface Sci.*, 1985, **156**, 678–700.
52 Z. P. Li, X. R. Duan, C. H. Liu and B. A. Du, *Anal. Biochem.*, 2006, **351**, 18–25.
53 Z. L. Jiang, Z. W. Feng, T. S. Li, F. Li, F. X. Zhong and J. Y. Xie, *Sci. China Ser. B*, 2001, **44**, 175–181.
54 D. H. Tian, Z. S. Qian, Y. S. Xia and C. Q. Zhu, *Langmuir*, 2012, **28**, 3935–3951.
55 Y. Li, P. Wu, H. Xu, H. Zhang and X. H. Zhong, *Analyst*, 2011, **136**, 196–200.
56 W. Leesutthiphonchai, W. Dungchai, W. Siangproh, N. Nagamrojnavanich and O. Chailapakul, *Talanta*, 2011, **85**, 870–876.